

# Learning Longitudinal Deformations for Adaptive Segmentation of Lung Fields from Serial Chest Radiographs\*

Yonghong Shi<sup>1</sup> and Dinggang Shen<sup>2</sup>

<sup>1</sup> Digital Medical Research Center, Fudan University, Shanghai, China 200032  
Yonghong.Shi@fudan.edu.cn

<sup>2</sup> Department of Radiology and Biomedical Research Imaging Center  
University of North Carolina, Chapel Hill, NC 27510  
dgshen@med.unc.edu

**Abstract.** We previously developed a deformable model for segmenting lung fields in serial chest radiographs by using both population-based and patient-specific shape statistics, and obtained higher accuracy compared to other methods. However, this method uses an *ad hoc* way to evenly partition the boundary of lung fields into some short segments, in order to capture the patient-specific shape statistics from a small number of samples by principal component analysis (PCA). This *ad hoc* partition can lead to a segment including points with different amounts of longitudinal deformations, thus rendering it difficult to capture principal variations from a small number of samples using PCA. In this paper, we propose a learning technique to adaptively partition the boundary of lung fields into short segments according to the longitudinal deformations learned for each boundary point. Therefore, all points in the same short segment own similar longitudinal deformations and thus small variations within all longitudinal samples of a patient, which enables effective capture of patient-specific shape statistics by PCA. Experimental results show the improved performance of the proposed method in segmenting the lung fields from serial chest radiographs.

**Keywords:** Statistical model, Active shape model, Hierarchical principal component analysis, Scale space analysis.

## 1 Introduction

Segmentation of lung fields in chest radiographs has been an active topic of research for over several decades, since chest radiograph is a popular diagnosis model to observe the dynamical behavior of the heart. However, the low signal-to-noise ratio (SNR) and the multiplicative nature of the noise (speckle) corrupting the chest radiograph make the segmentation of lung fields difficult [1-3]. We previously developed

---

\* This work is supported by Science and Technology Commission of Shanghai Municipality of China (Grant number: 06dz22103).

an algorithm of segmenting lung fields in serial chest radiographs by using both population-based and patient-specific shape statistics, and obtained higher accuracy compared to other methods [4]. However, this algorithm uses an *ad hoc* way to evenly partition the boundary of lung fields into some short segments, in order to capture the patient-specific shape statistics from a small number of samples by using hierarchical principal component analysis (*hierarchical PCA*) [5]. In particular, the boundary of lung fields is evenly partitioned into a number of short segments and then PCA is performed for each segment, as well as for the set of middle points of all segments. This *ad hoc* partition can lead to a segment including points with different amounts of longitudinal deformations, thus rendering it difficult to capture principal variations from a small number of samples using PCA.

It would be very attractive to develop an optimal partition technique to replace the *ad hoc* partition in our algorithm, thus the variation in each short segment can be assumed to be linear and thus can be better captured by PCA. In this paper, we develop a learning technique to adaptively partition the boundary of lung fields into short segments according to the longitudinal deformations learned for each boundary point. Therefore, all points in the same short segment own similar longitudinal deformations and thus small variations within all longitudinal samples of a patient, which enables effective capture of patient-specific shape statistics by PCA. Experimental results show the improved performance of the proposed method in segmenting the lung fields from serial chest radiographs.

This paper is organized as follows. In Section 2, we first summarize the whole framework of our previous segmentation algorithm, and then describe a technique to learn longitudinal deformations from online acquired longitudinal samples and use them to adaptively partition the boundary of lung fields by using a scale space analysis method. The performance of this improved lung field segmentation method is demonstrated in Section 3. This paper concludes in Section 4.

## 2 Method

### 2.1 Summary of Our Previous Segmentation Algorithm

For segmenting lung fields from serial clinical chest radiographs, we have developed a deformable segmentation model using both population-based and patient-specific shape statistics [4]. This model demonstrated better accuracy in segmenting serial chest radiographs, compared to other model-based segmentation methods. There are two novelties in this algorithm. *First*, a more distinctive local descriptor, referred to as scale invariant feature transform (SIFT) [6], is used to characterize the image features in the vicinity of each pixel, thus allowing the deformable model to accurately match correspondences in the image. *Second*, two types of shape statistics are used to guide the deformable model. In particular, for segmenting the *initial* time-point images, the population-based shape statistics is mainly used to guide the deformable model. As more subsequent longitudinal images are acquired from the same patient, the patient-specific shape statistics is collected from the previous segmentation results, and used to guide the deformable model. This patient-specific shape statistics is updated each time when a new segmentation result is obtained, and the updated patient-specific

shape statistics is further used to refine the segmentation of all available time-point images. When a sufficient number of longitudinal images are acquired and segmented from the same patient, the patient-specific shape statistics is considered sufficient to completely capture the variability of lung fields in the specific patient, without the need of using population-based shape statistics for the segmentation of future time-point images. Experimental results confirm that the use of this patient-specific shape statistics yields more robust and accurate segmentation of lung fields for serial chest radiographs.

However, to capture patient-specific shape statistics from a small number of longitudinal samples, the boundary of lung fields is currently partitioned into short segments using an *ad hoc* way. This *ad hoc* partition can lead to a segment including points with different amounts of longitudinal deformations, thus rendering it difficult to capture principal variations from a small number of samples using PCA. To overcome this limitation, we develop a learning technique to adaptively partition the boundary of lung fields into short segments according to the learned longitudinal deformations for each boundary point. This results in each short segment having similar longitudinal deformations, thus enabling the effective capture of patient-specific shape statistics by PCA. The details of our proposed technique are provided in the next subsection.

## 2.2 Adaptive Boundary Partition Using the Learned Longitudinal Deformations

To demonstrate the importance of learning the longitudinal deformations to guide the adaptive partition of lung field boundary, we *first* summarize our previous *ad hoc* partition method and point out its limitations by giving a visual example. Then, we will provide the details of our learning-based method for achieving adaptive partition of lung field boundary according to the learned longitudinal deformations.

### ***Ad hoc* boundary partition for capturing patient-specific shape statistics**

At time-point  $t$ , we have  $t-1$  previously segmented images and a current time-point image  $I_t$ . We can use the  $t-1$  segmentation results from the images  $I_1, \dots, I_{t-1}$ , as the training samples, to capture the patient-specific shape statistics. For effectively capturing the shape statistics from a small number of longitudinal samples of the same patient, we adopt a hierarchical representation of shape statistics, namely *Hierarchical PCA*. In particular, we partition the contours along the boundaries of lung fields into  $G$  overlapping segments, each of which consists of  $g$  contour points. The top level of the contours consists of  $G$  middle points of  $G$  segments, reflecting the spatial relationships between different segments, while the bottom level has  $G$  segments, each with  $g$  contour points to capture local shape changes. If  $g$  is comparable with the number of longitudinal samples, *i.e.*,  $t-1$ , statistical variation of each segment might be well captured by this number of samples. Thus, by computing the local shape statistics for each segment and also the global shape statistics for the  $G$  middle points of  $G$  segments, we might be able to capture both local and global shape variation information from the longitudinal samples using  $G+1$  PCA models.

Fig. 1(a) shows an example of evenly partitioning the boundaries of lung fields into 9 segments by our previous method. Also, the longitudinal variation of each boundary point is visualized by an ellipse that indicates both the directions and the amounts of

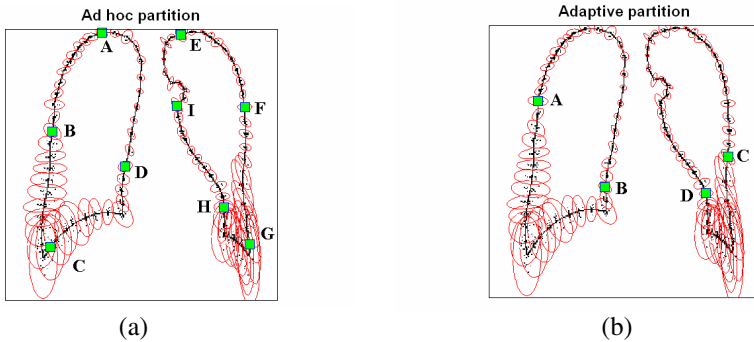


**Fig. 1.** Illustration of the importance of performing adaptive boundary partition, to allow each segment to have the points with similar longitudinal deformations

longitudinal deformations. It can be observed that there exist large longitudinal deformations for the bottom parts of lungs. The locations of points C and G are not reasonably placed in partition of boundaries of lung fields into nine segments. In particular, the segments CD and FG include points with different longitudinal deformations, which make it difficult to capture the statistical variations from a small number of samples by PCA. On the other hand, by using the learning technique developed in this paper, we can obtain optimal partition of boundaries according to the learned longitudinal deformations. For example, four segments are partitioned in Fig. 1(b), each having points with similar longitudinal deformations.

### ***Adaptive partition for capturing patient-specific shape statistics***

To adaptively partition the boundaries of lung fields into a number of short segments, we first learn the statistical variations for each point in the boundaries. We particularly use a PCA to capture the longitudinal deformation for each point from all available longitudinal samples of a specific patient. For example, for a patient image shown in Fig. 2(a), longitudinal deformation for each point is shown by a corresponding ellipse in Fig. 2(b). The long and short axes of the ellipse represent the major and the secondary directions of longitudinal deformation, and the size of ellipse represents the amount of longitudinal deformation. Figs. 2(c) and (d) show respectively the amounts of principal longitudinal deformation for each boundary point on the boundaries of right and left lungs. This information can be used as a reasonable foundation for adaptive partition of boundaries of lung fields.

However, the curves of principal longitudinal deformation (Figs. 2(c) and 2(d)) have many local details, as also shown in Figs. 3(b) and (d) by blue dashed curves. For determining the best partition positions, a scale space analysis technique, which can decide the parts to be smoothed out and the amount of smoothing, is used to approximate each curve by smoothing out only small details [7]. In this way, the approximated curve represents the global shape of a given curve. For example, as shown in Figs. 3(b) and (d), with the increase of scale, the curvature of the approximated curve becomes more even and constant, as demonstrated by pink, light blue, red and

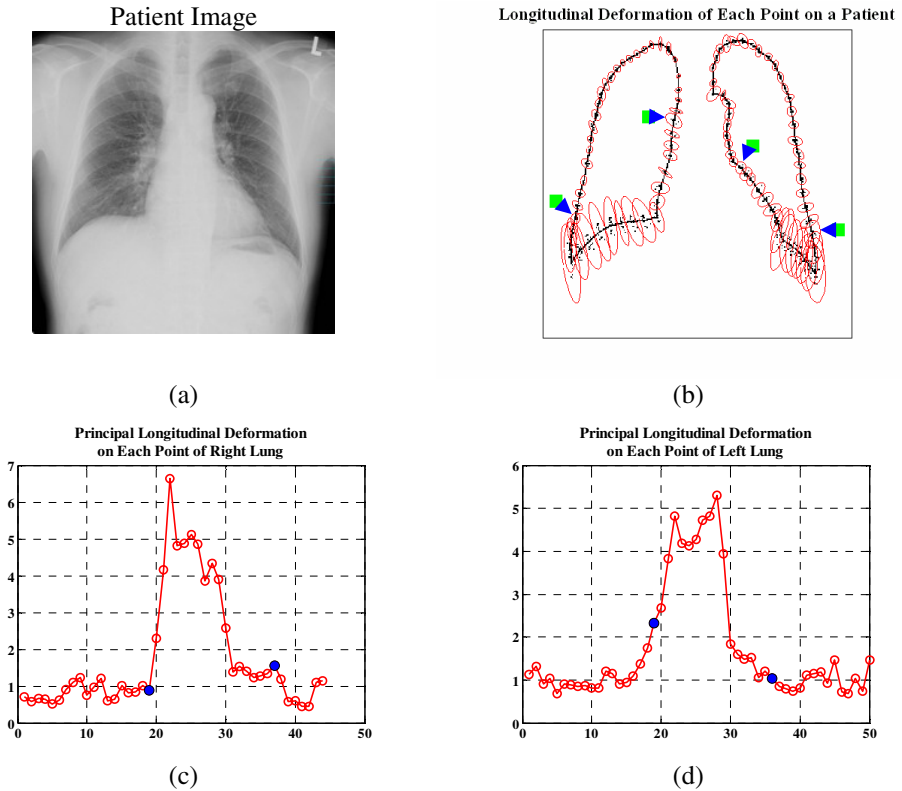


**Fig. 2.** Demonstration of longitudinal deformation of each point on the boundaries of right and left lungs of a patient

green curves, respectively. Then, the inflection points, i.e., the zero-crossings of second derivatives of the curve, can be used to judge the best partition positions of optimal subparts of the curve. When we plot the inflection points at every scale on the scale space, we can obtain so-called the finger print patterns. For example, in Figs. 3(a) and (c), different colors correspond to different scales, and as the scale increases from pink to light blue, red and green, the number of the inflection points decreases. Note, the scale space is spanned by the original position and the scale, for easy comparison across results from different scales.

It is known that the inflection points disappear only when two or more inflection points meet together in the scale space. Therefore, the finger print pattern closes upward as shown in Figs. 3(a) and (c). We define a shape segment as a part of a given contour between two inflection points which meet together when they disappear. As the scale increases, the number of shape segments decreases, and finally no shape segment remains. In Figs. 3(b) and (d), green curves correspond to the largest scale we used, and the green triangles indicate the inflection points which partition the curve into segments, i.e., with stronger and weaker longitudinal deformations. Finally, when we map these inflection points to the original contours of lung fields, we can

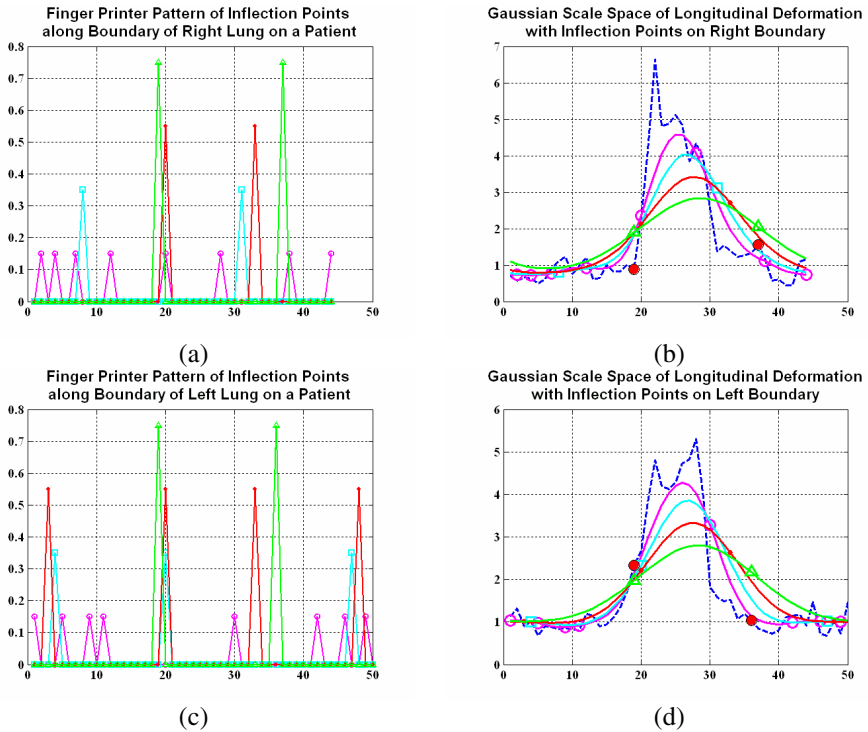


**Fig. 3.** Detecting the inflection points on the scale space of the leaned longitudinal deformation curves, for optimal boundary partition. *This figure is best viewed with color.*

acquire the optimal partition positions as blue triangles in Fig. 2(b). The advantage of using this adaptive partition technique for better capturing the patient-specific shape statistics is demonstrated in the experiments below.

### 3 Experiments

Various experiments are performed to evaluate the performance of our improved algorithm in segmenting the serial frontal chest radiographs of 39 patients. Most of these 39 patients have up to 17 monthly scanned images, each with 256x256 pixels. The lung fields of all these serial images have been manually delineated by a human observer, thus these manual segmentation results can be used as a golden standard to evaluate the segmentation results obtained by our method and all other methods in [4]. Two quantitative measures are used to evaluate the performance of the segmentation algorithm, i.e., the average overlay percentage and the average contour distance between automated segmentation result and manual segmentation result [4].

In order to objectively evaluate the performance of our algorithm, we compare the following five segmentation methods. *Method 1* is our complete method, which uses SIFT features, population-based shape statistics, and patient-specific shape statistics captured by *Adaptive* boundary partition. *Method 2* uses *ad hoc* boundary partition to

replace *Adaptive* boundary partition in *Method 1* to capture patient-specific shape statistics. *Method 3* is similar to *Method 2*, except that *Method 3* uses *global PCA*, without partition on the patient lung field boundaries, to directly estimate patient-specific shape statistics. In addition, the *ASM SIFT*, which is our method without using patient-specific shape statistics, and the *ASM Intensity*, which is the standard ASM algorithm [3, 4], are also compared in this paper.

The average overlay percentages and the average contour distances of all the five methods are shown in Table 1 and Table 2, respectively. It can be observed that the average overlay percentage of *Method 1* (95.0%), *Method 2* (94.9%) and *Method 3* (94.8%) that use patient-specific shape statistics are much higher than that of *ASM SIFT* (91.0%) and *ASM Intensity* (87.3%). Similar conclusion can be drawn for the average contour distance in Table 2. All of these results indicate that the methods using the patient-specific shape statistics (*Methods 1~3*) outperform those without using patient-specific shape statistics (*ASM SIFT* and *ASM Intensity*). On the other hand, the use of SIFT features improves the segmentation performance, e.g., *ASM SIFT* is better than *ASM Intensity*.

Furthermore, by comparing the results obtained by *Methods 1-3* in Tables 1 and 2, it can be observed that the use of boundary partition (*Method 1-2*) performs better than no partition on patient's lung field boundaries (*Method 3*), when used to capture

**Table 1.** Average overlay percentage between manual segmentation and automated segmentation by five methods on the serial chest radiographs database of 39 patients (%)

Algorithm	Mean $\pm$ std	Minimum	Median	Maximum
<i>Method 1</i> (Adaptive boundary partition)	95.0 $\pm$ 1.2	90.3	95.2	97.0
<i>Method 2</i> (Ad hoc boundary partition)	94.9 $\pm$ 1.3	88.4	95.0	97.0
<i>Method 3</i> (No boundary partition)	94.8 $\pm$ 1.4	88.2	95.1	96.9
<i>ASM SIFT</i>	91.0 $\pm$ 1.7	85.0	91.4	94.8
<i>ASM Intensity</i>	87.3 $\pm$ 4.9	76.9	89.2	93.7

**Table 2.** Average contour distance between manual segmentation and automated segmentation by five methods on the serial chest radiographs database of 39 patients. (Unit in pixel)

Algorithm	Mean $\pm$ std	Minimum	Median	Maximum
<i>Method 1</i> (Adaptive boundary partition)	1.05 $\pm$ 0.26	0.58	1.01	2.12
<i>Method 2</i> (Ad hoc boundary partition)	1.10 $\pm$ 0.31	0.62	1.06	2.72
<i>Method 2</i> (No boundary partition)	1.10 $\pm$ 0.30	0.62	1.07	2.75
<i>ASM SIFT</i>	2.06 $\pm$ 0.46	1.06	1.97	3.76
<i>ASM Intensity</i>	3.07 $\pm$ 1.35	1.32	2.45	6.05

the patient-specific shape statistics from a small number of longitudinal samples of the same patient.

Finally, the use of adaptive partition (*Method 1*) produces better segmentation results than the use of ad hoc partition (*Method 2*). For example, the average overlay percentage is increased from 94.9% to 95.0%, and standard deviation is reduced from 1.3% to 1.2%. In the meanwhile, the minimum overlay percentage is increased from 88.4% to 90.3%. Similarly, we can see the average contour distance is decreased from 1.10 to 1.05 pixels, and the standard deviation is decreased from 0.31 to 0.26 pixel. In the meanwhile, the minimum, median, maximum contour distances are all greatly decreased by using adaptive boundary partition.

## 4 Conclusion

We have developed an improved method for segmenting boundaries of lung fields from serial chest radiographs. The better performance is achieved by the improved collection of patient-specific shape statistics using adaptive boundary partition according to the learned longitudinal boundary deformations. In the current paper, only the amount of principal longitudinal deformation is used to guide the boundary partition. In the future, we will include both the direction and the amount of principal longitudinal deformations to guide the partition of lung field boundaries. This can potentially make each resulting segment have not only similar amount of longitudinal deformation but also similar direction of longitudinal deformation, thus enabling better capture of patient-specific shape statistics for guiding the lung field segmentation.

## References

1. van Ginneken, B., ter Haar Romeny, B.M., Viergever, M.A.: Computer-Aided Diagnosis in Chest Radiography: a Survey. *IEEE Trans. On Medical Imaging* 20(12), 1228–1241 (2001)
2. van Ginneken, B., Stegmann, M.B., Loog, M.: Segmentation of Anatomical Structures in Chest Radiographs using supervised methods: a Comparative Study on a Public Database. *Medical Image Analysis* 10, 19–40 (2006)
3. Cootes, T.F., Taylor, C.J.: Statistical Models of appearance for Computer Vision. Technical Report, Wolfson Image Analysis Unit, University of Manchester (2001)
4. Shi, Y., Qi, F., Xue, Z., Chen, L., Ito, K., Matsuo, H., Shen, D.: Segmenting Lung Fields in Serial Chest Radiographs Using Both Population-based and Patient-specific Shape Statistics. In: Larsen, R., Nielsen, M., Sparring, J. (eds.) *MICCAI 2006*. LNCS, vol. 4190, pp. 83–91. Springer, Heidelberg (2006)
5. Davatzikos, C., Tao, X., Shen, D.: Hierarchical Active Shape Models Using the Wavelet Transform. *IEEE Trans on Medical Imaging* 22(3), 414–423 (2003)
6. Lowe, D.G.: Distinctive Image Features from Scale-Invariant Keypoints. *International Journal of Computer Vision* 60(2), 91–110 (2004)
7. Hontani, H., Deguchi, K.: Primitive Curve Generation Based on Multiscale Contour Figure Approximation. In: *Proceeding of 15th International Conference on Pattern Recognition*, vol. 2, pp. 887–890 (2000)